Applied Geochemistry 48 (2014) 16–27

Contents lists available at ScienceDirect

Applied Geochemistry

journal homepage: www.elsevier.com/locate/apgeochem

Mobilization of selenium from the Mancos Shale and associated soils in the lower Uncompahgre River Basin, Colorado

M. Alisa Mast [a,*], Taylor J. Mills [a], Suzanne S. Paschke [a], Gabrielle Keith [a], Joshua I. Linard [b]

[a] U.S. Geological Survey, Colorado Water Science Center, Denver, CO 80225, United States
[b] U.S. Geological Survey, Colorado Water Science Center, Grand Junction, CO 81506, United States

ARTICLE INFO

Article history:
Available online 5 July 2014
Editorial handling by M. Kersten

ABSTRACT

This study investigates processes controlling mobilization of selenium in the lower part of the Uncompahgre River Basin in western Colorado. Selenium occurs naturally in the underlying Mancos Shale and is leached to groundwater and surface water by limited natural runoff, agricultural and domestic irrigation, and leakage from irrigation canals. Soil and sediment samples from the study area were tested using sequential extractions to identify the forms of selenium present in solid phases. Selenium speciation was characterized for nonirrigated and irrigated soils from an agricultural site and sediments from a wetland formed by a leaking canal. In nonirrigated areas, selenium was present in highly soluble sodium salts and gypsum. In irrigated soils, soluble forms of selenium were depleted and most selenium was associated with organic matter that was stable under near-surface weathering conditions. Laboratory leaching experiments and geochemical modeling confirm that selenium primarily is released to groundwater and surface water by dissolution of highly soluble selenium-bearing salts and gypsum present in soils and bedrock. Rates of selenium dissolution determined from column leachate experiments indicate that selenium is released most rapidly when water is applied to previously nonirrigated soils and sediment. High concentrations of extractable nitrate also were found in nonirrigated soils and bedrock that appear to be partially derived from weathered organic matter from the shale rather than from agricultural sources. Once selenium is mobilized, dissolved nitrate derived from natural sources appears to inhibit the reduction of dissolved selenium leading to elevated concentrations of selenium in groundwater. A conceptual model of selenium weathering is presented and used to explain seasonal variations in the surface-water chemistry of Loutzenhizer Arroyo, a major tributary contributor of selenium to the lower Uncompahgre River.

Published by Elsevier Ltd.

1. Introduction

Selenium (Se) is a major contaminant of concern in surface water in the lower Uncompahgre River Basin (LURB), which drains into the Colorado River system in western Colorado. Selenium is naturally present in Cretaceous Mancos Shale and is leached to groundwater and surface water by agricultural and domestic irrigation and leakage from irrigation canals (Butler et al., 1996; Butler and Leib, 2002; Bureau of Reclamation, 2011). Upstream from major irrigated areas, surface-water concentrations in the Uncompahgre River are low (<1 μg L^{-1}) whereas downstream from irrigated areas concentrations often exceed the aquatic life standard of 4.6 μg L^{-1} (Butler and Leib, 2002). Loutzenhizer Arroyo, a tributary of the Uncompahgre River (Fig. 1), has some of the greatest Se concentrations in the basin with concentrations as high as 345 μg L^{-1} during the winter baseflow period (http://waterdata.usgs.gov/nwis). Dissolved Se in surface water accumulates through the aquatic food chain, and its toxic effects can result in mortality, decreased reproduction, and deformities in offspring of fish and birds (Lemly, 1985; Ohlendorf et al., 1986; Luoma and Presser, 2009). Selenium concentrations in endangered Colorado pikeminnow (*Ptychocheilus lucius*) and razorback sucker (*Xyrauchen texanus*) in the Colorado River downstream from the LURB were found to be twice the recommended toxic threshold guideline and it was suggested that Se might be affecting reproductive success and survival of young (Osmundson et al., 2000).

Selenium has four oxidation states (VI, IV, 0, −II) in the environment and all can occur together in soils and sediments (McNeal and Balistrieri, 1989; Wright et al., 2003). Selenate (VI) is the most soluble form of Se and is chemically similar to sulfate (SO_4^{-2}) forming bonds with divalent cations (Aruga, 1978). In alkaline and oxidizing conditions typical of soils in the LURB, selenate is the dominant form and likely occurs in soluble salts or substituted

* Corresponding author. Tel.: +1 303 236 6898; fax: +1 303 236 4912.
E-mail address: mamast@usgs.gov (M.A. Mast).

http://dx.doi.org/10.1016/j.apgeochem.2014.06.024
0883-2927/Published by Elsevier Ltd.

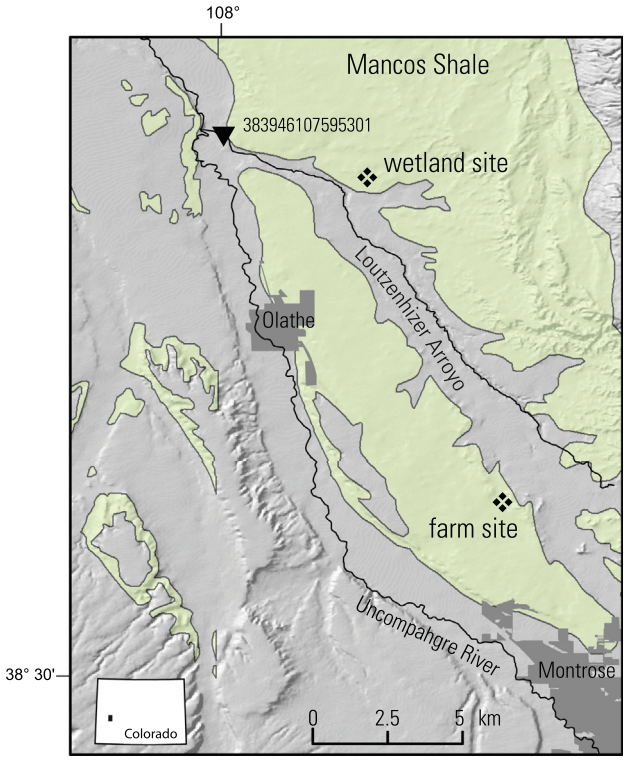

Fig. 1. Study site locations, major drainages, and areas underlain by Mancos Shale in the lower Uncompahgre River Basin.

for SO_4^{-2} in gypsum or carbonate in calcite (Tuttle et al., 2014). Selenite (IV) is a less soluble form that tends to sorb to clays, metal oxides, and organic matter in the pH range of 5–8 (Balistrieri and Chao, 1990; McNeal and Balistrieri, 1989; Boult et al., 1998). Selenite adsorption increases with decreasing pH and it is the dominant form in neutral or slightly acidic soils (Balistrieri and Chao, 1990; Maryland et al., 1991). The reduced inorganic forms, selenide (−II) and elemental Se (0), have low solubility and low bioavailability. Selenium also is assimilated biologically and much of the reduced Se in wetland sediments is associated with organic matter (Zhang and Moore, 1996). In deep unweathered cores of the Mancos Shale, Se primarily occurs as selenide substituted for sulfide in pyrite (Tuttle et al., 2014).

In the western U.S., weathering of Se bearing geologic formations mainly releases Se as selenate (Presser, 1994), but mobility of Se through soil and groundwater systems also can be controlled by redox conditions (White et al., 1991; Bailey et al., 2012). Under highly reducing conditions, Se is microbially reduced to insoluble forms, which diminishes concentrations in groundwater. Selenium reduction was documented at the Kesterson Reservoir in California where anoxic bed sediments in ponds provided a redox barrier that sequestered Se and prevented transport of Se to the underlying groundwater system (White et al., 1991). Under mildly reducing to oxidizing conditions, Se remains mobile in groundwater and can eventually be transported to surface water. Nitrate (NO_3^-) plays an important role in Se mobility because it has a greater redox potential than selenate. Thus, if sufficient dissolved NO_3^- is present, Se as selenite and selenate will remain in solution even if oxygen is depleted (White et al., 1991; Gates et al., 2009). Based on this NO_3^- redox control, previous work suggests that application of fertilizer in agricultural areas might enhance Se release and mobility from irrigated soils (Wright, 1999; Gates et al., 2009; Bailey et al., 2012). Previous studies have reported high NO_3^- concentrations in undisturbed soils in arid regions (Walvoord et al., 2003) including soils developed in Mancos Shale (Holloway and Smith, 2005; Morrison et al., 2012) suggesting that naturally occurring soil NO_3^- also may play a role in Se mobilization from soils.

Multiple local, State, and Federal agencies, including the Bureau of Reclamation and the U.S. Geological Survey (USGS), have worked to quantify the effects of Se on water quality, aquatic wildlife, and birds in the Upper Colorado River Basin including the LURB and to reduce Se loads to surface water through implementation of best management practices (Bureau of Reclamation, 2011). However, processes controlling mobilization of Se from Cretaceous marine shale in this region, including the Mancos Shale, are not fully understood. An approach, combining field data and laboratory studies with geochemical mass balance and conceptual models, was used to examine the processes influencing the mobilization of Se in the LURB.

2. Materials and methods

2.1. Soils and well core sediments

Shallow soil cores (<150 cm) were collected at a farm just north of Montrose, Colorado (Fig. 1) using a truck-mounted soil corer (5 cm diameter). One core was collected in an irrigated hay field (IR) and a second was collected on an adjacent hillslope that had never been irrigated or cultivated (NIR). The NIR core was deeply weathered whereas the IR core penetrated into minimally weathered shale within 30 cm of the surface. In this part of the study area, flat lying alluvial deposits, which typically are cultivated, are punctuated by small hills that are not cultivated where the bedrock is at or very close to the surface. Sediments also were collected from drill cores taken from a small wetland near Olathe, Colorado (Fig. 1). The 10 ha wetland was formed by leakage from an unlined irrigation canal. The canal has been in operation nearly 100 years (http://www.usbr.gov/projects/Project.jsp?proj_Name=Uncompahgre+Project) and delivers water primarily during the irrigation season (April–October). A 10 cm diameter core was collected using a hollow-stem auger during installation of groundwater monitoring wells (WM, WS) (Fig. S1 in online supplement). The WM well is located in the middle of the wetland (total depth 8.8 m) and the WS well is located at the toe of the wetland (total depth 11.6 m). A shallow core (total depth 2.7 m) also was collected at a site (DH) adjacent to the wetland but outside the area wetted by the leaking canal. All drill cores penetrated into shale bedrock that was weathered to various degrees. Solids were air dried, crushed, and sieved to less than 2 mm. Soil samples were combined by horizon and the sediment cores were combined over 75-cm depth intervals. Each composite was dissolved with a mixture of nitric, hydrofluoric, and perchloric acids and analyzed for total Se by hydride generation/atomic fluorescence spectroscopy (HG-AFS) (Briggs and Crock, 1986). A few well-formed gypsum crystals in the samples also were analyzed for total Se. For a subset of samples, heavy minerals were separated by sonication and panning and examined for pyrite under a binocular scope. Five samples were analyzed for stable N isotopes at the USGS Stable Isotope Laboratory (http://isotopes.usgs.gov/).

2.2. Sequential extractions

Sequential extractions were conducted on the soils and core sediments to determine the operationally-defined forms of Se in solid phases using the protocol described by Kulp and Pratt (2004). The sequence of extractions includes (1) a deionized water extraction for soluble Se, (2) a 0.1 mol L^{-1} K_2HPO_4–KH_2PO_4 buffer for adsorbed and exchangeable Se, (3) a 0.1 mol L^{-1} NaOH extraction for base-soluble organic Se (humic and fulvic acids), (4) a 1 mol L^{-1} Na_2SO_3 extraction for elemental Se, and (5) and 15% ace-

Table 1
Sediment mixes used in column experiments.

Mix	Description	Depth
NIR	Nonirrigated soil	0–96 cm
IR	Irrigated soil	0–150 cm
DH	DH core	1.2–2.7 m
WM-U	WM core upper section	1.2–7.3 m
WM-L	WM core lower section	7.3–8.8 m
WS-U	WS core upper section	1.2–4.9 m
WS-L	WS core lower section	4.9–11.6 m

tic acid extraction for Se associated with carbonates. A subset of samples also was extracted with 5% NaOCl, which can oxidize organic matter not extracted by the NaOH step (Wright et al., 2003). Following each extraction, samples were centrifuged and filtered through 0.45 μm syringe filter then transferred to 60-ml bottles for analysis. The water, phosphate, and NaOH extracts were analyzed for selenite and total Se (selenate equals total Se minus selenite for this analysis) and the other extracts were analyzed for total Se only. For the analysis, an aliquot of the extract was diluted to 25 ml with 10% HCl and the selenite concentration was measured by HG-AFS. A second aliquot was digested with a mixture of nitric, hydrochloric, and perchloric acid to convert all forms of Se to selenite prior to analysis by HG-AFS (Briggs and Crock, 1986). Aliquots from the water extraction also were analyzed for chloride (Cl^-), NO_3^- and SO_4^{-2} by ion chromatography (IC). Acidified aliquots were analyzed for major and trace elements by inductively coupled plasma-atomic emission spectrometry (ICP-AES). To test for reproducibility, 15% of samples were extracted in duplicate. Data for sequential extractions and chemical analyses are provided in Tables S1 and S2 in the online supplement.

2.3. Laboratory leaching studies

For the column experiments, the sediments and soils were further combined into seven sediment mixes including upper and lower composites for the WM and WS cores and composites of all depths for the DH core and the IR and NIR soils (Table 1). The leaching of Se from the mixes was investigated using polyethylene columns that were 20 cm in length with a diameter of 1.5 cm. Each column was filled with 70–80 g of solids at a uniform density that was capped on each end with 2 cm of quartz sand and a glass wool plug. Because of the high clay content of the sediment, quartz sand had to be mixed with the sediments in order to maintain flow through the column; a 50:50 mix of quartz sand and sediment was used after trying several different proportions. The inflow solution, which was deionized water, was gravity fed through the column from the bottom up to avoid preferential flow. Two sets of experiments were conducted (short and long duration). The short-duration experiments were conducted with all 7 sediment mixes and the long-duration experiments were conducted with the NIR, WS-L, WM-L, and DH mixes (Table 1). The short duration experiments were conducted to test the effect of wetting and drying cycles on release rates, which in the field could be related to water table fluctuations. In the short duration experiment, six pore volumes of input solution were passed through each column and collected in aliquots of one pore volume each. For each sediment mix, two identical columns were leached separately, and the aliquots were combined to produce sufficient leachate for all analyses. The number of pore volumes was computed as the volume of water passed through the column divided by the pore volume, which was estimated from the sediment mass, column volume, and an assumed density of 2.65 g cm^{-3}. After the initial leaching step, the material was extruded from the column and dried overnight at 30 °C. The dried material was lightly crushed and repacked in a column. The leach was repeated on the dried sediment by passing an additional six pore volumes through the dried material. In the long-duration experiments, one pore volume of input solution was passed through the column after which the flow was stopped until the next day. This process was repeated 9 more times yielding 10 aliquots for each experiment. Three different input solutions were used in the long-duration experiments, the first was oxygenated deionized water, the second was oxygen-free deionized water, and the third treatment was oxygen-free deionized water with 100 mg L^{-1} NO_3^- as N. To prepare the solutions, oxygen was removed from deionized water by boiling followed by purging with N_2 gas overnight. N_2 was bubbled through the input solution during the entire duration of the experiments. Nitrate was added using $NaNO_3$ salt.

Aliquots from all experiments were filtered and refrigerated for later analysis. Leachates were analyzed for selenite and total Se (detection limit 0.2 μg L^{-1}) on acidified (pH < 2 with HCl) aliquots by HG-AFS and anions were analyzed on unacidified aliquots by IC (Tables S3 and S4 in online supplement). Leachates from the short duration experiments were analyzed for major cations and trace elements by ICP-AES. One blank column (sand only) and one replicate column of the NIR soil were run to test for contamination and reproducibility.

2.4. Geochemical model

Groundwater chemistry in the wetland was modeled using PHREEQC (Parkhurst and Appelo, 2013) to improve understanding of the weathering reactions controlling Se release from the Mancos Shale. Batch-reaction calculations in PHREEQC were used to calculate dissolved Se concentrations based on forward-equilibrium reactions and inverse modeling. Forward equilibrium-reaction calculations bring a solution to thermodynamic equilibrium with defined reactants (Parkhurst and Appelo, 2013). Inverse modeling uses a set of user-defined mole transfers of phases and reactants and accounts for changes in water chemistry along a flow-path. The WATEQ4F database was used for all thermodynamic data except $CaSeO_4$, for which thermodynamic data were obtained from Cornelis et al. (2008). Two separate scenarios were simulated using canal water as the input solution and adding reactants to match the groundwater chemistry. Scenario I used forward-equilibrium calculations to investigate mineral sources of dissolved Se and scenario II used inverse modeling to identify probable modern weath-

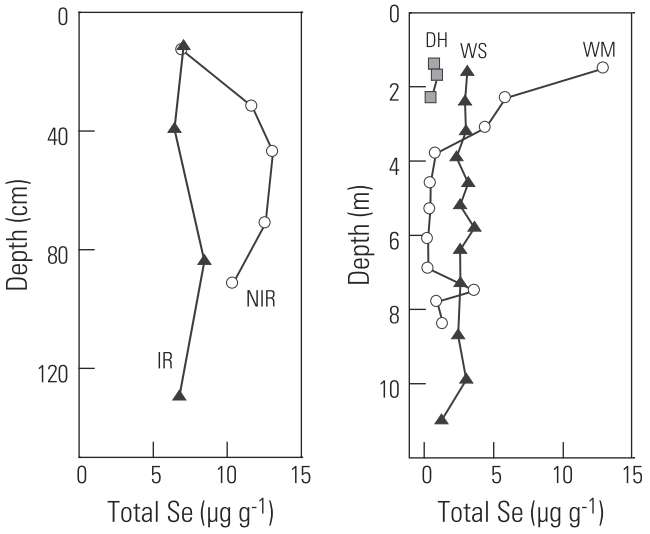

Fig. 2. Depth profiles of total selenium concentrations in agricultural soils (IR and NIR) and wetland sediments (DH, WM, WS).

ering reactions controlling groundwater chemistry. Water-chemistry data for East Canal (USGS station number 384016107574601) and groundwater at well WS (USGS station number 383858107572301) were obtained from the USGS National Water Information System (NWIS) database (http://waterdata.usgs.gov/nwis). Solid phases of Se in wetland sediments were represented as a solid solution with selenate substituted for SO_4^{-2} in gypsum ($Ca[SeO_4,SO_4]$-$2H_2O$) and as highly soluble Na_2SeO_4 salt. Dissolved CO_2 gas concentration was set at equilibrium with a partial pressure of 10^{-2} atmospheres and equilibrium was maintained with calcite and CO_2 throughout the simulations.

3. Results

3.1. Chemistry of soils and wetland sediments

3.1.1. Total chemistry

Total Se in the NIR soil profile averaged 10.9 μg g^{-1} and increased with depth reaching a maximum of 13.1 μg g^{-1} below 40 cm, whereas total Se in the IR soil was lower averaging 7.1 μg g^{-1} and concentrations were relatively uniform with depth (Fig. 2, Table S1). In the wetland, total Se in the solid phases varied little with depth in the WS well and shallow DH core. In the WM core, concentrations were greatest near the land surface (12.9 μg g^{-1}) and decrease with depth (Fig. 2). Pyrite in heavy mineral separates was only detected in one of the 21 samples examined indicating little pyrite from the original Mancos Shale remains in soils and wetland sediments collected for this study. This is consistent with the finding of Tuttle et al. (2014) who reported pyrite was largely absent in the upper 3 m of undisturbed weathering profiles in the Mancos Shale landscapes.

3.1.2. Water exchangeable anions

The depth profiles of water-extractable anions showed considerable variability among sites (Fig. 3, Table S2). Chloride, NO_3^-, and SO_4^{-2} generally increased with depth in the NIR soil and concentrations were greater in all horizons compared to the IR soil. The patterns for the wetland cores were more complex. Chloride was least in the bedrock core (DH) and showed little variability with depth. Chloride concentrations in the WM core were low near the surface but increased with depth. In contrast, Cl^- in the WS core was greatest near the surface, decreased to a minimum concentration around 4 m depth then increased again towards the bottom. In both WM and WS cores, NO_3^- was lowest near the surface and increased with depth to concentrations similar to those measured in the bedrock core (DH). Sulfate concentrations were similar

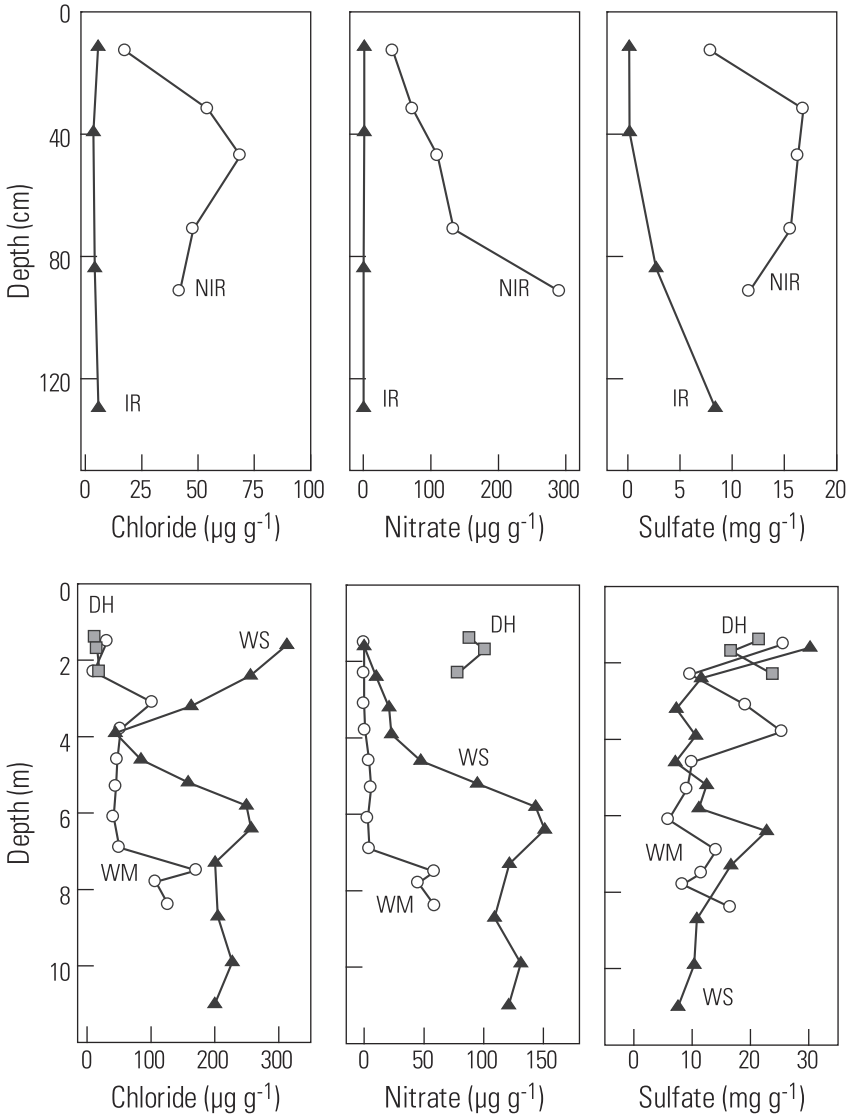

Fig. 3. Depth profiles of water extractable Cl^-, NO_3^- as N, and SO_4^{-2} concentrations in agricultural soils (IR and NIR) and wetland sediments (DH, WM, WS).

among sites and showed weaker patterns with depth compare to Cl^- and NO_3^-.

3.1.3. Sequential extractions

The analysis of Se speciation in solid phases is important because Se mobility and bioavailability are dependent on its chemical form (Zawislanski et al., 2003). Table S1 shows distribution of Se based on sequential extraction results for the soils and sediments collected by this study. Selenium recovery from the 5 fractions used in this study ranged from 3% to 100% with an average of 9% for the IR soil, 34% for the WS and WM cores, 54% for NIR soil, and 90% for DH core. Possible forms of residual Se not recovered by the extractions include metal selenide/sulfide minerals and Se associated with residual organic matter.

Water-extractable Se accounted for 1.3 to 80% of the total Se in soils and sediments, and concentrations in the NIR soil were nearly an order of magnitude greater than the IR soil and wetland sediments (Fig. 4). The majority of water-extractable Se was determined to be selenate, with less than 5% occurring as selenite. Phosphate extractable Se, which represents the adsorbed and exchangeable Se, accounted for 1–7% of the total Se with the greatest concentration also in the NIR soil (Table S1). Selenite accounted for a much larger fraction of dissolved Se (up to 82%) in the phosphate extraction, reflecting stronger adsorption of selenite than selenate to oxides, clay minerals, and organic matter (Zawislanski et al., 2003). Base-extractable Se, which includes inorganic and organic species bound to soil organic matter, ranged from 1% to 14% of total Se and was greatest in the NIR soil and lowest in the DH core. Less than 1% of the total Se was extracted in the $NaSO_3$ step indicating little Se in the study sediments is present in the elemental form. However, because the samples were air dried and sieved, the possibility that some reduced Se was oxidized during sample processing cannot be ruled out. Se in carbonates, based on the acetic acid extraction, was low in all soils and sediments ranging from 1% to 2% of the total Se. As a final step, samples from the WM core were extracted by NaOCl, which is shown to be efficient at oxidizing organic matter in soils (Wright et al., 2003). This fraction accounted for 7% of total Se in the WM core indicating a significant fraction of residual Se remained in the sediments likely bound in selenide/sulfide minerals or possibly residual forms of organic matter not fully oxidized by the NaOCl treatment.

The depth profiles for water-extractable Se are presented in Fig. 4. In the NIR soil, concentrations showed a 5-fold increase from the surface to the deeper horizons reaching concentrations over 6 μg g^{-1}. By contrast, concentrations in the IR soil were very low (<0.2 μg g^{-1}) and showed only a slight increase towards the bottom of the profile. In the WM core, the water-extractable Se profile was similar to NO_3^- with low concentrations near the surface and greater concentrations near the bottom. In the WS core, the Se profile followed the pattern of Cl^- rather than NO_3^-. Concentrations were greatest at the surface and bottom of the core and showed a minimum in the middle between depths of 3.5 and 4.9 m.

3.2. Column leachates

In all column experiments, Se levels were greatest in the initial pore volume then declined rapidly to relatively low levels in later stages of the experiments (Fig. S2 in online supplement). The NIR mix had the greatest Se concentrations in the initial pore volume reflecting the large concentration of water-extractable Se in the soil samples (Table S1). Most of the Se in the column leachates was present as selenate although selenite accounted for as much as 15% of the Se released from the NIR mix. Release rates for the short duration experiments were computed as ng of Se per g of soil per day and were calculated for the initial leaching period (excluding the first two pore volumes) and for the period after the sediment was dried (Table 2). The NIR mix has the greatest release rate, which was 6–7 times greater than that from the IR mix. For the wetland sediments, the WS-U mix had the greatest release rate and WM-L the lowest. Drying had a mixed effect on the release rate of Se from the soils and sediments (Fig. S3 in online supplement). Lower rates after drying were observed for NIR, IR, and WS-U mixes perhaps indicating some experiments had not yet reached steady state after 6 pore volumes because concentrations were still declining. In the DH mix, drying increased the rate of release largely due to a marked increase in flow rate after drying. Based on the replicate column for the NIR mix, reproducibility of rates determined after drying may be poor. Sulfate was the dominant anion released during the short-term experiments and calcium (Ca^{+2}) and sodium (Na^+) were the dominant cations. In the NIR soil, Na^+ concentrations were initially very high and approximately balanced SO_4^{-2} concentrations (Fig. 5). As leaching progressed, Na^+ concentrations decreased rapidly and Ca^{+2}, which increased only slightly, was the main cation balancing SO_4^{-2} at the end of the experiment. All the wetland sediment mixes (DH, WM-L, WM-U, WS-L, and WS-U) showed similar cation and SO_4^{-2} patterns to the NIR mix. In the IR mix, Ca^{+2} nearly balanced SO_4^{-2} through the entire experiment and there was only a small release of Na^+ in the first pore volume. In the NIR mix, Se was more strongly correlated with Na^+ ($r^2 = 0.96$) than with Ca^{+2} ($r^2 = 0.31$), and in the IR mix, Se was more strongly correlated with Ca^{+2} ($r^2 = 0.88$) than with Na^+ ($r^2 = 0.57$).

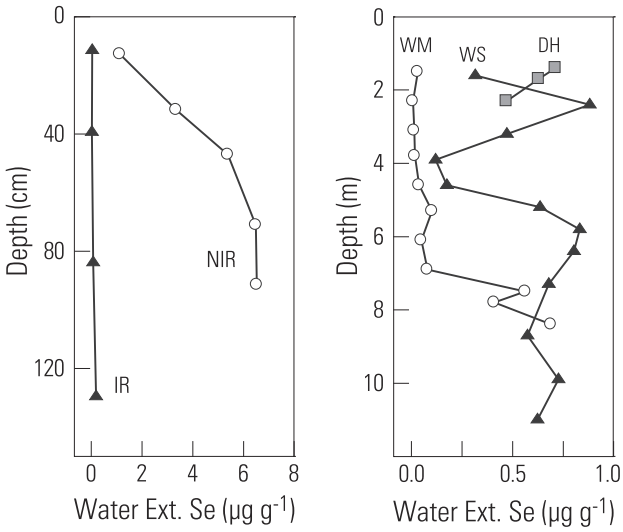

Fig. 4. Depth profiles of water extractable selenium concentrations in agricultural soils (IR and NIR) and wetland sediments (DH, WM, WS).

In the long-duration experiments, Se concentrations typically leveled off and reached a steady state after about 3 days. Average concentrations during steady state ranged from 0.4 μg L^{-1} for the WM-L mix up to 26 μg L^{-1} for the NIR mix. Release rates were computed as ng of Se per g of soil per day based on a linear fit of the reaction time versus the cumulative mass of Se released excluding the first 4 pore volumes collected during the experiment (Fig. S4 in online supplement). Steady-state rates for Se ranged from 0.30 to 33.8 ng g^{-1} d^{-1} (Table 2). Rate constants for the production of Se in the long-duration experiments were computed using a first-order reaction model (Stillings and Amacher, 2010), which yielded rate constants ranging from 0.001–0.006 d^{-1}. These values are similar to the values of 0.0007–0.0048 d^{-1} reported for batch experiments using the Mancos Shale (Wright, 1999) but less than values of 0.091–0.173 d^{-1} reported for batch experiments with the Niobrara Shale (Bailey et al., 2012). The three different treatments (oxygen saturated, oxygen free, oxygen free plus

Table 2
Release rates of selenium and sulfate in short duration experiments before and after drying and in long-duration experiments under conditions of dissolved oxygen (DO), oxygen free plus nitrate (NO3) and oxygen free (NDO) [–, no data].

	Short duration				Long duration					
	Se (ng g^{-1} d^{-1})		SO_4^{-2} (mg g^{-1} d^{-1})		Se (ng g^{-1} d^{-1})			SO_4^{-2} (mg g^{-1} d^{-1})		
Mix	Before	After	Before	After	DO	NDO + NO3	NDO	DO	NDO + NO3	NDO
NIR	437	188	14.7	8.6	33.8	31.8	29.4	1.8	1.8	1.7
NIR rep	434	305	13.5	15.0	–	–	–	–	–	–
IR	58.9	29.6	5.0	2.2	–	–	–	–	–	–
DH	8.9	47.6	5.1	61.3	1.2	1.2	1.2	1.6	1.6	1.4
WM-U	6.4	11.2	3.4	7.4	2.2	–	–	1.5	–	–
WM-L	1.2	5.8	1.3	1.9	0.30	0.32	0.33	0.28	0.21	0.24
WS-U	174	36.3	6.9	9.5	–	–	–	–	–	–
WS-L	7.8	12.8	2.6	8.8	1.4	1.5	1.9	0.97	0.95	1.0

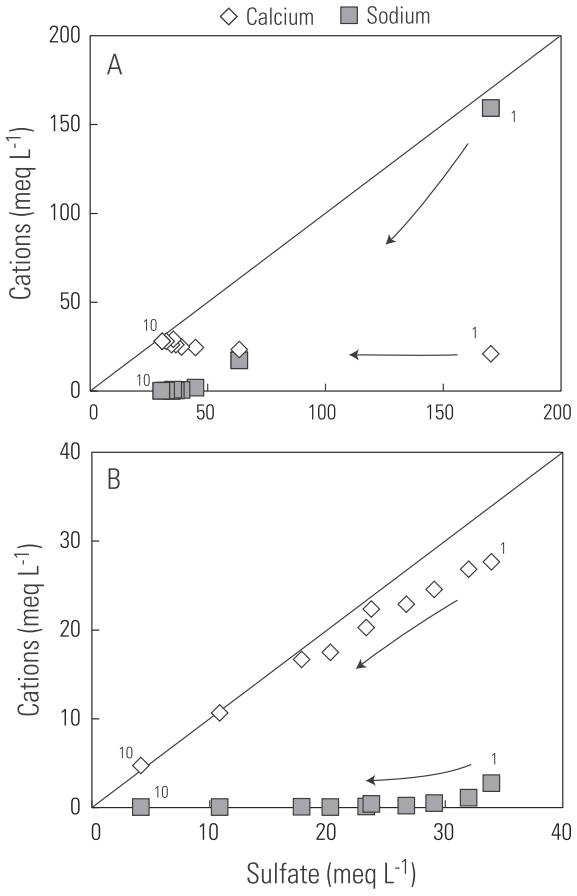

Fig. 5. Sulfate versus Ca^{+2} and Na^+ concentrations in short-duration experiments using (A) nonirrigated and (B) irrigated agricultural soils. Numbers indicate pore volumes passed through the sediment column and arrows indicate progression of leaching experiment.

NO_3^-) showed similar release rates (Fig. S5 in online supplement). For the NIR, DH, and WS-L sediments, SO_4^{-2} reached a steady-state concentration in the range of 1300–1500 mg L^{-1} at the end of each experiment in contrast to the WM-L sediment, which had a SO_4^{-2} concentration around 200 mg L^{-1}. Sulfate release rates ranged from 0.21 to 1.81 mg g^{-1} d^{-1} (Table 2) and were positively correlated with Se release rates.

3.3. Geochemical modeling

Scenario I used the canal water as the starting water composition and the resulting solution composition after reaction was compared to the water composition measured at the WS well, which is located at the down gradient end of the wetland. The groundwater had very high specific conductance (47,600 μS cm^{-1}), low dissolved oxygen (0.97 mg L^{-1}), and elevated concentrations of Se (4105 μg L^{-1}) and NO_3^- (823 mg L^{-1}). The canal water was very dilute compared to the groundwater at WS with a conductance of 986 μS cm^{-1} and a Se concentration of 9.6 μg L^{-1}. The canal water is sourced from the Gunnison River and is likely always considerably more dilute than the groundwater at WS.

Pyrite and gypsum are both present in the unweathered Mancos shale and have been proposed as possible sources of Se in soil (Morrison et al., 2012). However, pyrite is largely oxidized in the weathered Mancos and is unlikely to be the current source of Se in these soils and sediments. Scenario I was conducted to determine if gypsum is a plausible source of Se in the weathered Mancos Shale. In this scenario, Se-bearing gypsum was represented as an ideal solid solution between gypsum and $CaSeO_4$. In PHREEQC, the activity of each end-member solid phase in a solid solution is equal to its mole fraction and the different solubility of each phase is taken into account during dissolution of the solid solution (Parkhurst and Appelo, 2013). A Se concentration of 9 mg kg^{-1} was assigned to the gypsum-$CaSeO_4$ solid solution based on measurements of Se in a few crystals taken from the soil. In groundwater, divalent cations such as Ca^{+2} can exchange with Na^+ bound to clays in marine shale. Therefore, exchangeable Na^+ (NaX) on clays also was added as a reactant and represents the primary source of dissolved Na^+ in groundwater. Exchange of Ca^{+2} for Na^+ on exchange sites removes Ca^{+2} from solution, allows more gypsum-$CaSeO_4$ to dissolve, and represents a maximum gypsum-$CaSeO_4$ dissolution end-member. Scenario I allowed gypsum-$CaSeO_4$ to react with canal water until the solution reached saturation with respect to the solid-solution.

The simulation for scenario I overestimated the Na^+ and SO_4^{-2} concentration and underestimated the Ca^{+2} concentration (Table S5 in online supplement). The overestimated Na^+ and SO_4^{-2} and underestimated Ca^{+2} concentrations are caused by a surplus of Na^+ exchange sites binding Ca^{+2}, releasing Na^+, and driving excess gypsum dissolution resulting in high SO_4^{-2} values. Nevertheless, even under this maximum gypsum-$CaSeO_4$ end-member simulation, Se concentrations were still underestimated by nearly an order of magnitude. The results from scenario I are also consistent with observations from column experiments. Selenium concentrations during column experiments decreased by more than an order of magnitude after the first pore volume, suggesting that the majority of the Se resides in a highly soluble salt. The results from scenario I and column experiments indicate gypsum-$CaSeO_4$ dissolution is unlikely to be the only source of Se in this study.

Scenario II used a mass-balance approach to account for changes in water composition between an initial solution (canal) and a final solution (groundwater) and was conducted assuming Se is present in Na_2SeO_4 salt as well as gypsum. Gypsum was not

Table 3
Inverse modeling results for scenario II. Input solution is canal water and final solution is groundwater at WS well [–, no data].

Solute	Solution (mmol L^{-1})		Phase transfers (mmoles)							
	Initial	Final	Calcite	$NaNO_3$	Gypsum	$MgSO_4$	K_2SO_4	Na_2SO_4	Halite	Na_2SeO_4
Ca^{+2}	2.85	10.8	4.05	–	4.16	–	–	–	–	–
Cl^-	0.20	34.9	–	–	–	–	–	–	34.4	–
K^+	0.10	1.53	–	–	–	–	0.58	–	–	–
Mg^{+2}	1.26	56.4	–	–	–	62.1	–	–	–	–
NO_3^-	0.00	29.2	–	62.4	–	–	–	–	–	–
Na^+	2.71	512	–	62.4	–	–	–	246	34.4	54.3[a]
SO_4^{-2}	3.57	279	–	–	4.16	62.1	0.58	246	–	–
Se	0.12[a]	42.6[a]	–	–	–	–	–	–	–	54.3[a]

[a] Se species in μmoles.

considered as a substantial source of Se based on scenario I and thus was not included as a Se bearing reactant. In best model fit for scenario II, the simulated groundwater concentrations were within 5% of concentrations measured at WS for all constituents. Dissolved Ca^{+2} is supplied by calcite and gypsum dissolution, and Na^+, magnesium (Mg^{+2}), potassium (K^+), SO_4^{-2}, NO_3^-, and Se are supplied primarily from the dissolution of salts (Table 3). These minerals and salts have been found in the Mancos Shale or overlying soils (Tuttle et al., 2014). These results also are consistent with observations during column experiments. In column experiments, the initial pore volume in the nonirrigated soil had high concentrations of major ions and Se, which declined substantially in the second pore volume. Concentrations of Na^+, NO_3^-, Cl^-, and Se declined by more than an order of magnitude and concentrations of Mg^{+2}, K^+, and SO_4^{-2} declined by about 2-fold between the first and second pore volumes. Modeling and column leachate results are consistent and indicate that a substantial portion of these elements reside in highly soluble salts that are readily flushed from the soil when water is applied. In contrast, Ca^{+2} exhibited less variability throughout the column-leaching experiment and actually increased slightly during the experiment indicating that Ca^{+2} is supplied by less soluble phases that persist throughout the experiment, such as calcite and gypsum. The results of scenario II indicate that SO_4^{-2} is supplied primarily from the dissolution of salts, and it is likely that these salts are also the source of Se. Selenium concentrations up to 230 mg g^{-1} have been measured in salts found in the Mancos Shale (Tuttle et al., 2014).

4. Discussion

4.1. Distribution of Se in soils at the agricultural site

Total Se concentrations for soils and sediments collected in this study were greatest in the NIR soil at the agricultural site and ranged from 6.97 to 13.1 μg g^{-1}. The NIR is a residual soil developed in the Smokey Hill Member of the Mancos Shale (Noe et al., 2013) and the bottom of the profile extends into minimally weathered shale. These concentrations were at the high end of total Se measured in a soil survey in the nearby Gunnison Gorge National Conservation Area, which reported a range from 0.2 to 12.1 μg g^{-1} (Tuttle et al., 2007). The soil survey reported that Se concentrations were somewhat erratically distributed geographically apparently reflecting differences in Se concentrations in the Mancos Shale (Tuttle et al., 2014). Sequential extractions from this study indicate 41% of the Se in the soil profile occurs as water-extractable selenate. Selenium likely was released during oxidation of pyrite in the unweathered Mancos Shale and accumulated over thousands of years in the arid soils as a trace element in soluble salts or substituted for SO_4^{-2} in gypsum although no distinct Se salts have been identified in soils or bulk shale in the area (Tuttle et al., 2014). A gypsum crystal from the C-horizon of the NIR soil yielded a Se concentration of 8.9 μg g^{-1} indicating Se also is associated with gypsum in some soils. The fraction of water-extractable selenate increases with depth to over 60% in the C-horizon, which could be caused by leaching from surface layers or volatilization by plants. Chloride and NO_3^- showed similar patterns suggesting leaching at the surface, however, the accumulation of highly soluble salts at depth indicates little to no water movement has occurred below the rooting zone (Walvoord et al., 2003). Some exchangeable selenite was found in the NIR soil although this accounted for only 5% of the total Se because of the high pH of soils which favors desorption (Balistrieri and Chao, 1990). About 40% of the Se in soils was not recovered by the sequential extractions indicating it is bound in selenide/sulfide minerals or is associated with insoluble forms of organic matter. Pyrite was not observed in the C-horizon sample, which along with the highly oxidizing conditions suggests residual Se is largely associated with insoluble forms of organic matter not readily decomposed under near-surface weathering conditions.

The high concentrations of extractable NO_3^- in the NIR soil were somewhat unexpected considering the soil had never been cultivated. Elevated NO_3^- concentrations have been reported in natural springs emanating from the Mancos Shale (Morrison et al., 2012) and extracts from undisturbed soils in the Gunnison Gorge National Conservation Area (Tuttle et al., 2007) suggesting N might be from geologic sources. Nitrogen in the Mancos Shale is largely organic with lesser amounts in NO_3^- salts and ammonium in clays

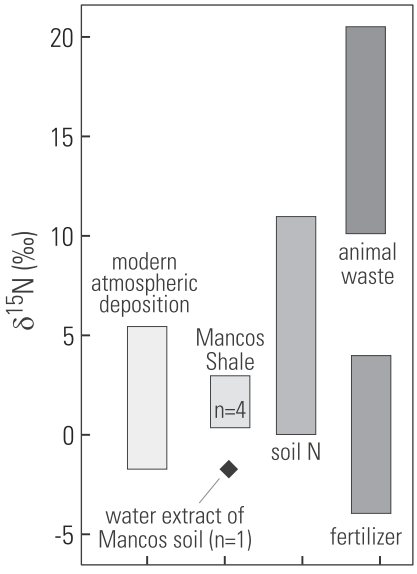

Fig. 6. Range of $\delta^{15}N$ values of potential sources of N in water extract from Mancos-derived soil. Range of values for atmospheric deposition from Nanus et al. (2008) and soil N, fertilizer, and animal wastes from Kendall (1998).

(Holloway and Smith, 2005). High concentrations of soluble soil NO_3^- can occur in arid soils due to a combination of low organic matter and water content, and highly aerobic conditions; all of which promote NO_3^- stability and inhibit denitrification (Walvoord et al., 2003). The $\delta^{15}N$ values were used to help infer the source of soluble NO_3^- in soil. The C-horizon of the NIR soil, which had the highest concentration of extractable NO_3^- (291 μg g^{-1}), had a $\delta^{15}N-NO_3^-$ value of −1.74‰ (Table S6 in online supplement). Total N concentrations in the four solid samples also were elevated (590 to 850 mg kg^{-1}) and $\delta^{15}N$ values were slightly heavier than the soil extract ranging from 0.99‰ to 2.50‰. Considering that only one sample of soil extract was measured, the range of $\delta^{15}N$ in the shale seems to be consistent with the extractable NO_3^- in soil although it is also near the lower end of the range of total N in natural soil (Fig. 6). Other potential sources of soil N are fertilizer, animal wastes, and atmospheric deposition (Fig. 6). Nitrate derived from animal wastes typically has $\delta^{15}N$ values between +10 and +20‰ (Kendall, 1998); too enriched to account for soluble NO_3^- in soil. Anthropogenic fertilizer overlaps the range of $\delta^{15}N$ measured in this study, however, there is little evidence the soils have been cultivated so this source should be minor. Modern atmospheric deposition in Colorado ranges from 5.5‰ to −2.0‰ (Nanus et al., 2008) and if it is not much different from that of pre-industrial deposition then it could account for some extractible NO_3^- in soils.

The IR soil profile was deeper and more highly weathered than the adjacent NIR soil likely because of decades of irrigation and the nature of the parent material, which has been described as clayey alluvium derived from Mancos Shale rather than shale bedrock (Fisher, 2005). The distribution of soluble Se and salts in the IR soil was very different from the NIR soils and clearly shows the effects of prolonged irrigation (Figs. 3 and 4). Irrigation also diminished concentrations of exchangeable Se in soil, which accounted for 1% of total Se in IR soil compared to 5% in the NIR soil. Assuming the pre-irrigation soil chemistry at IR was similar to the NIR soil, soluble and exchangeable forms of Se were almost entirely flushed from the soils by irrigation down to at least 150 cm. A mass balance for soluble/exchangeable Se indicates for every m^2 of cultivated land approximately 8.4 kg of Se have been removed since the site has been under irrigation. Assuming irrigation has occurred over 100 years, the value of 84 mg m^{-2} yr^{-1} is 3 times greater than 31 mg m^{-2} yr^{-1} estimated by Tuttle et al. (2014) for the Gunnison Gorge National Conservation Area. The value from this study might be an upper limit considering Se in the NIR soil is high relative to other undisturbed soils in the region (Tuttle et al., 2007). The majority of Se in the IR soil appeared to be associated with organic matter. Less than 10% of the Se was associated with labile forms of organic matter based on the NaOH extraction suggesting the remainder is in insoluble forms of organic matter. Kulp and Pratt (2004) reported as much as 50% of Se was not extractable in Cretaceous shale and inferred much of it was kerogen-bound organic Se complexes. The origin of residual Se in the IR soil is not clear. Residual Se (1.87 mg g^{-1}) in the minimally weathered C-horizon of the NIR soil (Fig. 7) suggests some may be associated with shale-derived kerogen. However, higher concentrations of residual Se in the upper soil horizons suggest that some Se was incorporated into organic matter accumulated through soil microbial processes. An important question is whether irrigation/cultivation promotes decomposition of organically bound Se potentially releasing it in soluble or bioavailable forms. Fig. 7 compares organically bound Se (NaOH and residual) concentrations in the IR and NIR soil profiles. NaOH extractable Se is depleted in the IR soils relative to NIR suggesting more weakly bound Se may be taken up by plants or is susceptible to decomposition (Lin and Norman, 2003). By contrast, residual Se in IR soil is comparable to or slightly greater in concentration than the NIR soil suggesting residual organic Se is relatively stable in this environment and may even act as a sink for Se in irrigated soils.

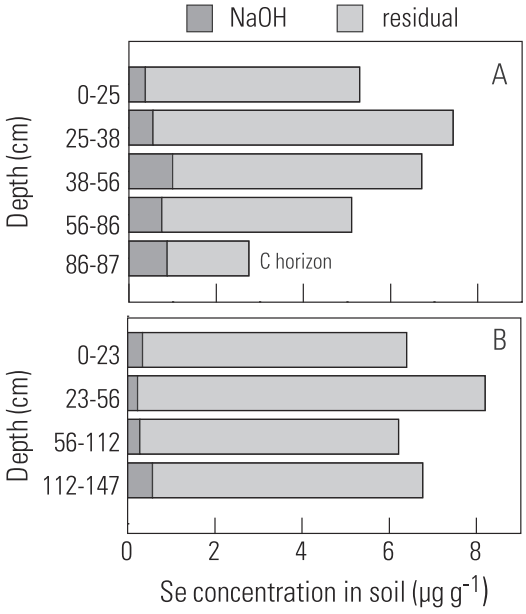

Fig. 7. Comparison of residual and NaOH extractable Se by horizon for the (A) nonirrigated and (B) irrigated agricultural soils.

4.2. Distribution of Se in sediments at the wetland site

Total Se concentrations in the wetland sediments are much less than in the agricultural soils likely reflecting variability in the Se content of the parent material, which also is mapped as the Smokey Hill Member of the Mancos Shale (Noe et al., 2013). The DH core penetrated minimally weathered shale very close to the surface whereas in the WM core, the upper 4 m was a clay-rich material with few if any remnants of the original shale. Below 4 m, subhorizontal weathered shale beds were present, which became harder and darker in color below 6 m. At the WM well there is a shallow perched groundwater system and vegetation is wetland grasses and sedges. A deeper water-bearing zone along bedding planes and weathering fractures occurred around 8 m. Sediment from the WS well was firm clay with few rock fragments down to around 2 m with weathered Mancos Shale below. A water bearing lens of sand was encountered at 9.5 m. Vegetation at WS was sagebrush rather than grasses indicating the well site is down gradient of the permanently saturated area.

Profiles of Se phases and water-extractable anions in the core sediments indicate that a combination of leaching, redox, and evaporation have altered the original Se geochemistry of the sediments in the wetland. The DH core was drilled into an undisturbed area and was collected to represent chemistry of underlying geologic materials in the wetland prior to canal leakage. In DH, the total Se was low (<1.0 μg g^{-1}) and nearly all Se was present in water-extractable forms (80%). In the WM core, water extractable Se is depleted to a depth of about 7 m as are the mobile anions NO_3^- and Cl^- (Figs. 3 and 4). These patterns suggest the upper 7 m of the sediment are leached by canal water, while sediments below this level have had minimal contact with infiltrating water. Assuming the water-extractable Se in WM sediments was initially the same as at DH, leakage from the canal may have removed up to 4.8 kg m^{-2} of Se from the sediment since it has been in operation (100 years). The wetland has not only been a source of Se but apparently also acts as a sink as evidenced by the large increase in total Se in the surface sediment at WM (Fig. 2). Little of this Se

was extracted in either the NaOH/NaOCl steps (organic Se) or the Na_2SO_3 step (elemental Se) suggesting it resides in metal selenide or sulfide minerals. Because the shallow groundwater has low dissolved oxygen and abundant SO_4^{-2}, it seems likely that pyrite or metal selenide formation in the anaerobic surface sediments is sequestering Se from shallow groundwater. The surface sediments at WM were examined under a scanning electron microscope but no sulfide or selenide minerals were detected. High Se concentrations (up to 90 μg g^{-1}) were reported in reducing sediments at the bottom of a small reservoir not far from the wetland, which were assumed to be in selenide phases based on the light isotopic composition of sulfur in the lake sediment (Tuttle et al., 2014). In the wetland, the amount of Se sequestered in the upper 3.4 m was estimated at nearly 30 kg m^{-2}. Because this is more than the amount lost by leaching of soluble salts from unweathered Mancos Shale, the Se may come from up gradient areas of the wetland or from the canal water, which has concentrations ranging from 7 μg L^{-1} during the irrigation season and up to 140 μg L^{-1} during the non-irrigation season. Based on Se inventories in the WM and DH cores, anaerobic surface sediments in some parts of the wetland may have sequestered more Se than has been leached from the unweathered bedrock since the canals were established. Because the results are for a single well core, however, these processes may not necessarily be occurring at other locations in the wetland.

Profiles of water-extractable Se and anions in the WS core were different from WM, reflecting its hydrologic position in the wetland (Figs. 3 and 4). At depths below 6 m, soluble Se as well as mobile anions Cl^- and NO_3^- are elevated relative to the surface indicating there has been minimal contact with groundwater. The WS well had higher total Se and Cl^- at depth than the DH core sediment possibly because of differences in parent material composition. Over the 4–6 m interval, concentrations of water-extractable Se, Cl^-, and NO_3^- in WS decline to concentrations similar to those in the upper part of the WM core indicating the sediment has been leached by groundwater. Close to the surface, however, the patterns diverge with soluble Se and Cl^- increasing toward the surface in the WS core compared to low concentrations near the surface of WM. A possible explanation is that shallow subsurface flow occasionally reaches the toe of the wetland where it can be evaporated and precipitate soluble salts. Nitrate content is low in the soluble salts because it presumably is removed up gradient of the well by biological uptake or reduction in the wetland. This hydrologic scenario is consistent with field observations in April 2013 when the saturated area increased to within 100 m of the WS well for a few weeks when the canal started flowing. The water retreated shortly after because of infiltration and increased rates of evapotranspiration as the growing season progressed. The total Se accumulated in near-surface sediments of WS was about 1.5 kg m^{-2} or about 30% of the soluble Se leached from Mancos Shale at WM.

4.3. Laboratory study of Se weathering

Initially high Se concentrations in the column leachate followed by a rapid decline in concentrations indicates that highly soluble forms of Se are initially released from the sediment followed by slower release from less soluble phases. As shown in the sequential extractions, Se in the study sediment is present in a number of different forms ranging from dominantly water-extractable forms in undisturbed (nonirrigated or leached) soils/sediments to residual forms in irrigated soils and wetland surface sediments. The high concentrations of Se along with Na^+ and SO_4^{-2} in the initial leachate indicates that Se is present in easily dissolved selenate salts or is substituted for SO_4^{-2} in the mineral thenardite (Na_2SO_4). Exchange reactions also may contribute some Se in the initial leachate; however, equilibrium should be reached as the leaching experiment progresses. Once steady-state is reached, Se release is controlled by less soluble phases. Some laboratory studies have demonstrated that longer-term release is governed by oxidation of more refractory species such as elemental Se and Se associated with sulfides (Zawislanski and Zavarin, 1996; Stillings and Amacher, 2010). In this study, there was little evidence for the occurrence of either of these reduced forms and the residual Se likely is bound to organic matter. Zawislanski and Zavarin (1996) reported that organic Se was oxidized during laboratory studies but at a very slow rate compared to other reduced forms. In contrast to other studies, steady-state Se release measured in this study appears to be controlled by dissolution of gypsum even in the IR and WM-U sediments that have been subject to decades of irrigation or leaching. This is inferred from the positive correlation between Se and SO_4^{-2} release rates (r^2 = 0.89), and the major ion data, which shows Ca^{+2} and SO_4^{-2} are balanced in all the column leachates in the later stages of the reaction. Even in the highly leached soils (IR and WM-U), there is sufficient gypsum in the soil to produce steady-state SO_4^{-2} concentrations of about 200 mg L^{-1} in the column leachates. The ratio of Se (μg) to SO_4^{-2} (g) in the leachates ranged 0.72 for the DH sediment to 18.8 in the NIR soil. A few gypsum crystals were analyzed from the solids including one from the DH core with a Se to SO_4^{-2} ratio of 0.38 (0.21 μg g^{-1}) and one from the NIR soil that had a ratio of 15.9 (8.9 μg g^{-1}). The ratio in the gypsum crystals is close to the leachate providing additional evidence that gypsum dissolution is the main process controlling steady-state Se release in the columns.

Based on the simple column experiments described herein, there was not a clear effect of drying on the release rate of Se from Mancos soils and sediments although the experiments were of relatively short duration and did not investigate multiple cycles of drying and wetting. This result is consistent with Se being mobilized largely from oxidized phases (salts and gypsum) rather than reduced phases such as pyrite, elemental Se, or organic Se. In wetlands where reduced Se is present, falling water tables and drying of the sediment could oxidize reduced Se and make it available for mobilization when the water tables rise again. Tuttle et al. (2014) found high concentrations of reduced Se in reservoir bed sediments and wetland soils in the LURB and suggested Se could be released at highly accelerated rates when saturated sediments are dried and exposed to ambient weathering conditions. The greatest sediment Se concentration in this study was found in the wetland surface sediments (12.9 μg g^{-1}), which appeared to be in a reduced selenide form, although this could not be confirmed. In the column experiments, Se release rate was about 5 times faster in the WM-U sediment compared to the WM-L sediment in the short duration experiments, which could indicate that some reduced Se was mobilized by oxidation. The release rate, however, was low compared to gypsum weathering in the NIR soil (0.44 ng g^{-1} d^{-1}) indicating residual Se was not easily oxidized during the experiment. Based on the sequential extractions, there also was little evidence that reduced Se was converted to oxidized forms during collection, drying, and sieving of the original core material. Zawislanski and Zavarin (1996) reported that reduced forms of Se in sediment deposited under strongly reducing conditions remained largely insoluble after the soils had been drained for more than 5 years due to low net Se oxidation rates. In the laboratory, the reduced Se was oxidizable but only under elevated temperature conditions (Zawislanski and Zavarin, 1996). Although Se appeared to be sequestered in the wetland sediment it was difficult to extract and did not appear to be readily mobilized under oxidizing conditions in the laboratory.

The long duration experiments investigated the effect of NO_3^- on Se release rates from the study soils and sediments. Studies have shown that presence of NO_3^- in groundwater induces mildly oxidiz-

ing conditions and inhibits microbial reduction of Se, thus permitting mobilization in groundwater (Weres et al., 1990; White et al., 1991). Oxygen and NO_3^- in groundwater also may enhance Se release by oxidizing reduced mineral forms of Se such as pyrite in shale bedrock (Wright, 1999; Bailey et al., 2012). In this study no differences were found between the three different treatments, which included oxygen saturated water, oxygen-free water, and oxygen-free water with 100 mg L^{-1} of NO_3^-. Rates for the three treatments for four sediment mixes are shown in Table 2. The similarity in release rates among the treatments largely reflect the lack of reduced mineral forms of Se in the sediments and the dominance of soluble oxidized phases, which should largely be controlled by solubility constraints. Alternatively, if some oxygen remained in the input solutions, the same rates could be produced in all three experiments.

Our results are different from those of Wright (1999) who conducted batch experiments with Mancos Shale collected in the LURB. The author reported increased Se release rates with increasing NO_3^- concentrations in the absence of oxygen suggesting NO_3^- enhanced Se release through oxidation of reduced phases (elemental Se and pyrite) from the Mancos Shale. In studies by Tuttle et al. (2014) in the same area, there is little evidence that primary pyrite remains in the upper 3 m of Mancos Shale landscapes so the question arises as to whether pyrite oxidation was the main reaction releasing Se in the experiments conducted by Wright (1999). Bailey et al. (2012) also conducted laboratory studies to investigate the effect of NO_3^- on oxidation of Se in the Cretaceous Niobrara Shale in eastern Colorado and concluded that autotrophic nitrification of pyrite was a major driver in the release of Se and SO_4^{-2} from the shale. Solids used in the Bailey et al. (2012) study were obtained from shallow boreholes (<16 m) drilled into shale bedrock. Mineralogy and Se content of bedrock samples used by Wright (1999) and Bailey et al. (2012) were not provided, however, complicating comparison with the results from this study.

Although the importance of NO_3^- on Se release rates from reduced phases in the study area is unclear, NO_3^- likely plays a role in inhibiting chemical reduction of oxidized forms of Se in the groundwater resulting in enhanced leaching and transport to surface water. Bailey et al. (2012) found that NO_3^- concentrations as low as 5 mg L^{-1} were enough to inhibit reduction of selenate in the groundwater. Analysis of soils and sediment in this study indicates that high concentrations of soluble NO_3^- salts are present in undisturbed soils and minimally weathered Mancos Shale, which when wetted, rapidly release NO_3^- to groundwater, as evidenced by the NO_3^- concentration greater than 300 mg L^{-1} in the WS well. In the irrigated soils and wetland surface sediments, soluble salts were depleted and no longer appeared to be a major source of NO_3^- to groundwater.

5. Conceptual model of Se mobilization from the Mancos Shale

Combining information on the distribution of Se in soils and sediments and results of the column experiments, together with the wetland hydrology and groundwater chemistry, allows us to build a conceptual model of Se release and mobilization to ground and surface water in the study area. The most mobile forms of Se are in highly soluble Na_2SO_4 salts and gypsum in naturally weathered Mancos Shale and derived materials. These salts have formed from the oxidation of pyrite in shale over thousands of years of weathering in the arid and highly oxidizing conditions in western Colorado (Tuttle et al., 2014). There is little evidence of primary pyrite remaining from the original Mancos Shale in near-surface weathering environments. Reduced forms of Se in soils and sediments likely are associated with organic matter in soils and bedrock. There is an abundance of soluble NO_3^- salts in the soil and sediment samples analyzed by this study presumably derived from oxidation of organic matter in the original shale. In the irrigated field and in the wetland, decades of irrigation and canal leakage have leached the highly soluble Se and NO_3^- salts out of soils and near surface sediments. Selenium is still released after the initial leaching of salts but at a much lower rate largely controlled by gypsum dissolution. Virtually no leachable NO_3^- salts remains from the parent material in saturated areas. Soils at the very surface of the wetland were saturated and sufficiently anoxic to immobilize Se from the canal water or from up gradient areas of the wetland. The Se appeared to be accumulating in a reduced form such as pyrite although the exact form could not be identified. There was little evidence that redox conditions were causing Se to accumulate in irrigated soils.

In contrast to the surface soils in the wetland, soluble Se and NO_3^- salts still remained in sediments from the deeper part of the core suggesting there was minimal percolation of water from saturated areas above. A deeper groundwater system was encountered beneath the wetland, which might have developed from canal seepage along the bedrock interface, bedding planes, or weathering fractures in the bedrock. The groundwater chemistry beneath the wetland was characterized by exceptionally high Se, Na^+, SO_4^{-2}, and NO_3^- concentrations, which the PHREEQC modeling and laboratory experiments showed to be controlled by dissolution of highly soluble salts. Although the dissolved oxygen was low in groundwater beneath the wetland, elevated NO_3^- concentrations maintained mildly reducing conditions, which inhibited the reduction of Se allowing it to reach a maximum concentration of about 3 mg L^{-1}. The $\delta^{15}N$ values of total N in shale suggests NO_3^- in the wetland groundwater is derived from bedrock weathering rather than agricultural activities although contributions from atmospheric deposition cannot be ruled out based on the isotopic data.

The conceptual model presented above was used to help explain the observed seasonal pattern in stream-water chemistry at Loutzenhizer Arroyo (Fig. 8). Loutzenhizer Arroyo is a tributary of the Lower Uncompahgre River (Fig. 1) that contributes a large load of Se to the LURB (Leib et al., 2012). Chemistry and discharge data were retrieved from the USGS NWIS database (waterdata.usgs.gov) for Loutzenhizer Arroyo just above the confluence with the Uncompahgre River, USGS station 383946107595301 (Fig. 1). Examination of seasonal variability in discharge reveals the stream has a strong bimodal character with flows of about 15 cfs in winter (November–March) and flows of about 85 cfs during the summer irrigation season. Flow is remarkably uniform in each season especially when compared to discharge of the upper Uncompahgre River, which is controlled by natural snowmelt runoff (Fig. 8). A strong bimodal pattern also is apparent in the water chemistry with much greater concentrations during winter baseflow than during the summer irrigation season. Similar to discharge, concentrations are remarkably uniform in each season; for example, SO_4^{-2} concentrations in winter averaged 2620 mg L^{-1} with a standard deviation of 7% and Se averaged 158 μg L^{-1} with a standard deviation of 12%. Average concentrations during the summer irrigation season were 4 times lower for SO_4^{-2} (715 mg L^{-1}) and 5 times lower for Se (34 μg L^{-1}) than during the winter and also showed a narrow range of values in each season. Fewer analyses are available for NO_3^- but the same pattern is apparent with elevated concentrations (8.2 mg L^{-1}) in winter compared to concentrations (1.5 mg L^{-1}) during the irrigation season.

The decrease in stream-water concentrations during the summer-irrigation season is interpreted as dilution of groundwater baseflow from irrigation supply and return flows. Although groundwater levels decline and dissolved solids concentrations in groundwater increase during the winter non-irrigation season (Butler et al., 1996), groundwater baseflow to streams is maintained year round as evidenced by streamflow and chemical con-

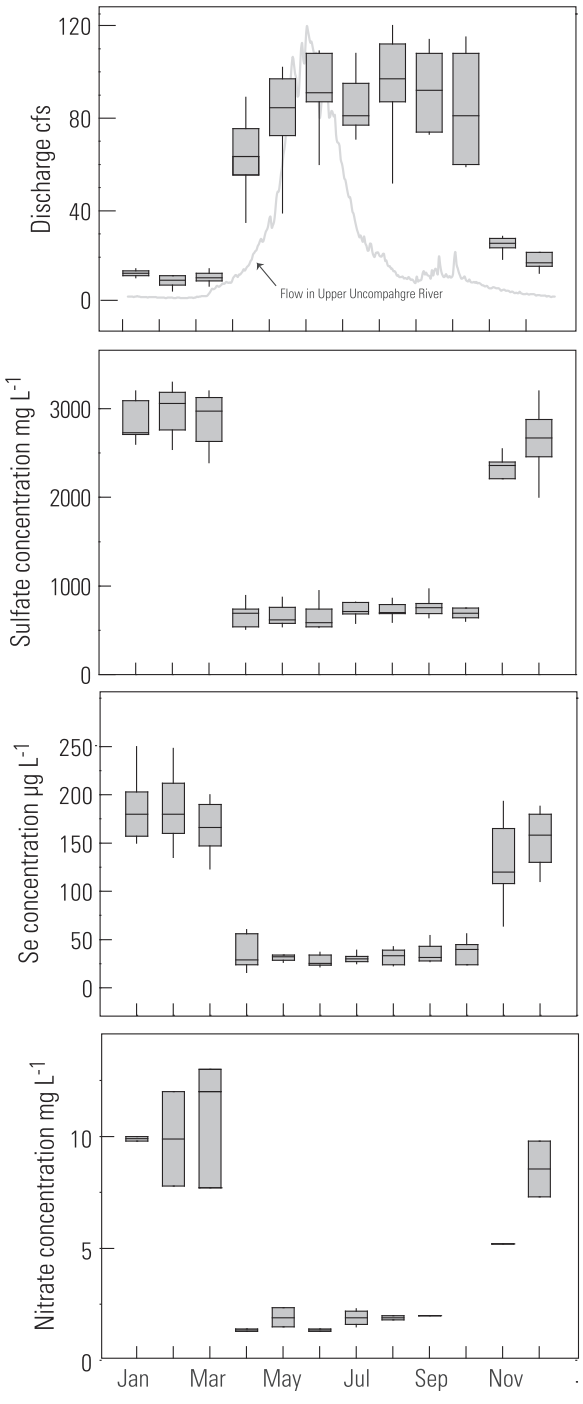

Fig. 8. Monthly variation in discharge, SO_4^{-2} ($n = 103$), Se ($n = 114$), and NO_3^- as N ($n = 24$) concentrations in Loutzenhizer Arroyo (1991–2013). Hydrograph of Uncompahgre River near Ridgeway (not to scale, station number 09146200, data for 2013 from USGS NWIS http://waterdata.usgs.gov/nwis), which is controlled by natural snowmelt, is included for comparison with flow at Loutzenhizer Arroyo, which is controlled by irrigation.

centration data for Loutzenhizer Arroyo (Fig. 8). During the winter non-irrigation season, groundwater levels and surface-water flow decline, resulting in continued weathering of less weathered bedrock at depth perhaps analogous to the preferential-path groundwater flow observed beneath the wetland. Once the irrigation season starts, flow increases rapidly and stabilizes through the summer because of surface runoff and deep percolation below the rooting zone from irrigated fields (irrigation recharge), returns flows, and leakage from unlined canals. An analysis of loading indicates 46–59% of the annual load of NO_3^-, SO_4^{-2} and Se occurs during the 5 winter months when recharge from irrigated fields to groundwater is minimal. Assuming the baseflow contribution of solutes remains constant during all months, the difference between summer-irrigation season loads and baseflow loads can be used to estimate solute concentrations in shallow groundwater or runoff generated from fields during the irrigation season. This approach yields concentrations of 0.1 mg L^{-1} for NO_3^-, 200 mg L^{-1} for SO_4^{-2} and 4 µg L^{-1} for Se. These values are remarkably similar to the leachate concentrations from the IR column experiments, which had a NO_3^- concentration of 0 mg L^{-1}, SO_4^{-2} of 200 mg L^{-1}, and Se of 3 µg L^{-1} once the column had reached steady state.

6. Conclusions

The results of field data, leachate experiments and geochemical modeling presented here suggest the NO_3^- in winter baseflow can be derived from naturally-occurring salts in the Mancos Shale rather than leaching of fertilizers applied to irrigated lands, although NO_3^- loading from irrigated fields is another potential source of N to surface water in the LURB. The concentrations of Se in baseflow suggest that NO_3^- maintains mildly oxidizing conditions in groundwater keeping Se in soluble forms and allowing transport to the surface-water system. Our data suggest that during irrigation season most water is contacting soils that have been leached by decades of irrigation and have relatively low capacity to release Se because Se-bearing soluble salts have been mostly leached from the soil. We believe the deep percolation of irrigation water and leakage from canals promotes groundwater flow through shallow bedrock along bedding planes and weathering fractures dissolving Se and NO_3^- from secondary salts. Dissolved NO_3^- from the dissolution of soluble salts plays an important role in keeping Se groundwater Se concentrations elevated by inhibiting selenate reduction.

Acknowledgements

This work was supported by funding from the Bureau of Reclamation Science and Technology Program. The authors thank Tracy Yager (U.S. Geological Survey) for assistance in the laboratory and Ken Leib (U.S. Geological Survey) and two anonymous reviewers for comments on a previous version of this manuscript.

Appendix A. Supplementary material

Supplementary data associated with this article can be found, in the online version, at http://dx.doi.org/10.1016/j.apgeochem.2014.06.024.

References

Aruga, R., 1978. Thermodynamics of association of selenate and sulfate with bivalent metals. Calculation, by calorimetric data, of the water molecules displaced from a cationic sphere. Inorg. Chem. 17, 2503–2505.
Bailey, R.T., Hunter, W.J., Gates, T.K., 2012. The influence of nitrate on selenium in irrigated agricultural groundwater systems. J. Environ. Qual. 41, 783–792.
Balistrieri, L.S., Chao, T.T., 1990. Adsorption of selenium by amorphous iron oxyhydroxide and manganese dioxide. Geochem. Cosmochim. Acta 54, 739–751.
Boult, K.A., Cowper, M.M., Heath, T.G., Sato, H., Shibutani, T., Yui, M., 1998. Towards an understanding of the sorption of U(VI) and Se(IV) on sodium bentonite. J. Contam. Hydrol. 35, 141–150.
Briggs, P.H., Crock, J.G., 1986. Automated Determination of Total Selenium in Rocks, Soils, and Plants. U.S. Geological Survey Open-File Report 86-40, 20p.
Bureau of Reclamation, 2011. Selenium Management Program Formulation Document Gunnison River Basin, Colorado, <http://www.usbr.gov/uc/wcao/progact/smp/docs/Final-SMP-ProgForm.pdf>.

Butler, D.L., Leib, K.J., 2002. Characterization of selenium in the Lower Gunnison River Basin, Colorado, 1988–2000. U.S. Geological Survey Water-Resources Investigations Report 02-4151, 26p.

Butler, D.L., Wright, W.G., Stewart, K.C., Osmundson, B.C., Krueger, R.P., Crabtree, D.W., 1996. Detailed Study of Selenium and Other Constituents in Water, Bottom Sediment, Soil, Alfalfa, and Biota Associated with Irrigation Drainage in the Uncompahgre Project area and in the Grand Valley, west-central Colorado, 1991–93. U.S. Geological Survey Water-Resources Investigations Report 96-4138, 136p.

Cornelis, G., Poppe, S., Gerven, T.V., den Broeck, E.V., Ceulemans, M., Vandecasteele, C., 2008. Geochemical modelling of arsenic and selenium leaching in alkaline water treatment sludge from the production of non-ferrous metals. J. Hazard. Mater. 159, 271–279.

Fisher, F.S., 2005. Uncompahgre River Basin Selenium Phytoremediation: Final Report for EPA Grant #WQC 01-00057, <http://www.seleniumtaskforce.org/phytoremediationproject.html>.

Gates, T.K., Cody, B.M., Donnelly, J.P., Herting, A.W., Bailey, R.T., Price, J.M., 2009. Assessing selenium contamination in the irrigated stream-aquifer system of the Arkansas River, Colorado. J. Environ. Qual. 38, 2344–2356.

Holloway, J.M., Smith, R.L., 2005. Nitrogen and carbon flow from rock to water: regulation through soil biogeochemical processes, Mokelumne River watershed, California, and Grand Valley, Colorado. J. Geophys. Res. 110, F01010. http://dx.doi.org/10.1029/2004JF000124.

Kendall, C., 1998. Tracing Nitrogen Sources and Cycling in Catchments. In: Kendall, C., McDonnell, J.J. (Eds.), Isotope Tracers in Catchment Hydrology. Elsevier, New York.

Kulp, T.R., Pratt, L., 2004. Speciation and weathering of selenium in Upper Cretaceous chalk and shale from South Dakota and Wyoming, USA. Geochim. Cosmochim. Acta. 68, 3687–3701.

Leib, K.J., Linard, J.I., Williams, C.A., 2012. Statistical Relations of Salt and Selenium Loads to Geospatial Characteristics of Corresponding Subbasins of the Colorado and Gunnison Rivers in Colorado. U.S. Geological Survey Scientific Investigations Report 2012-5003, 31p.

Lemly, A.D., 1985. Toxicology of selenium in a freshwater reservoir: implications for environmental hazard evaluation and safety. Ecotoxicol. Environ. Safety 10, 314–338.

Lin, Z.Q., Norman, T., 2003. Selenium removal by constructed wetlands: quantitative importance of biological volatilization in the treatment of selenium-laden agricultural drainage. Environ. Sci. Technol. 37, 606–615.

Luoma, S.N., Presser, T.S., 2009. Emerging opportunities in management of selenium contamination. Environ. Sci. Technol. 43, 8483–8487.

Maryland, H.F., Gough, L.P., Stewart, K.C., 1991. Selenium mobility in soils and its absorption, translocation, and metabolism in plants. In: Severson, R.C., Fisher, J.R., Scott, E., Gough, L.P. (Eds.), Proceeding of the 1990 Billings land Reclamation Symposium on Selenium in Arid and Semiarid Environments, Western United States. U.S. Geological Survey Circular 1064, pp. 57–65.

McNeal, J.M., Balistrieri, L.S., 1989. Geochemistry and occurrence of selenium: an overview. In: Jacobs, L.W. (Ed.), Selenium in Agriculture and the Environment. Soil Sci. Soc. Amer., Madison, Wisconsin, Special Publication no. 23, pp. 1–13.

Morrison, S.J., Goodknight, C.S., Tigar, A.D., Bush, R.P., Gil, A., 2012. Naturally occurring contamination in the Mancos Shale. Environ. Sci. Technol. 46, 1379–1387.

Nanus, L., Williams, M.W., Campbell, D.H., Elliott, E.M., Kendall, C., 2008. Evaluating regional patterns of nitrate sources to watersheds in national parks of the Rocky Mountains using nitrate isotopes. Environ. Sci. Technol. 42, 6487–6493.

Noe, D.C., Morgan, M.L., Townley, S.M., 2013. Olathe Northwest Quadrangle Geologic Map, Delta and Montrose Counties, Colorado. Colorado Geological Survey <http://geosurveystore.state.co.us/p-1455-olathe-northwest-quadrangle-geologic-map-delta-and-montrose-counties-colorado.aspx>.

Ohlendorf, H.M., Hoffman, D.J., Saiki, M.K., Aldrich, T.W., 1986. Embryonic mortality and abnormalities of aquatic birds: apparent impacts by selenium from irrigation drainwater. Sci. Tot. Environ. 52, 49–63.

Osmundson, B.C., May, T.W., Osmundson, D.B., 2000. Selenium concentrations in the Colorado pikeminnow (*Ptychocheilus lucius*) relationship with flows in the Upper Colorado River. Arch. Environ. Contam. Toxicol. 38, 479–485.

Parkhurst, D.L., Appelo, C.A.J., 2013. Description of input and examples for PHREEQC Version 3—A computer program for speciation, batch-reaction, one-dimensional transport, and inverse geochemical calculations. U.S. Geological Survey Techniques and Methods 6-A43, Chapter 43 of Section A, Groundwater Book 6, Modeling Techniques.

Presser, T.S., 1994. Geologic origin and pathways of selenium from the California Coast Ranges to the West-Central San Joaquin Valley. In: Frankenberger, W.T., Benson, S. (Eds.), Selenium in the Environment. Marcel Dekker Inc., New York, NY, 456p.

Stillings, L.L., Amacher, M.C., 2010. Kinetics of selenium release in mine waste from the Meade Peak Phosphatic Shale, Phosphoria Formation, Wooley Valley, Idaho, USA. Chem. Geol. 269, 113–123.

Tuttle, M.L.W., Fahy, J.W., Grauch, R.I., Ball, B.A., Chong, G.W., Elliott, J.G., Kosovich, J.J., Livo, K.E., Stillings, L.L., 2007. Results of chemical analyses of soil, shale, and soil/shale extract from the Mancos Shale Formation in the Gunnison Gorge National Conservation Area, southwestern Colorado, and at Hanksville, Utah. U.S. Geological Survey Open-File Report: 2007-1002-D.

Tuttle, M.L.W., Fahy, J.W., Elliott, J.G., Grauch, R.L., Stillings, L.L., 2014. Contaminants from Cretaceous black shale: I. natural weathering processes controlling contaminant cycling in Mancos Shale, southwestern United States, with emphasis on salinity and selenium. Appl. Geochem., 46, 57–71.

Walvoord, M.A., Phillips, F.M., Stonestrom, D.A., Evans, R.D., Hartsough, P.C., Newman, B.D., Striegl, R.G., 2003. A reservoir of nitrate beneath desert soils. Science 302, 1021–1024.

Weres, O., Bowman, H.R., Goldstein, A., Smith, E.C., Tsao, L., Harnden, W., 1990. The effect of nitrate and organic matter upon mobility of selenium in groundwater and in a water treatment process. Water Air Soil Pollut. 49, 251–272.

White, A.F., Benson, S.M., Yee, A.W., Wollenberg Jr., H.A., Flexser, S., 1991. Groundwater contamination at the Kesterson Reservoir, California: 2. Geochemical parameters influencing selenium mobility. Water Resourc. Res. 27, 1085–1098.

Wright, W.G., 1999. Oxidation and mobilization of selenium by nitrate in irrigation drainage. J. Environ. Qual. 28, 1182–1187.

Wright, M.T., Parker, D.R., Amrhein, C., 2003. Critical evaluation of the ability of sequential extraction procedures to quantify discrete forms of selenium in sediments and soils. Environ. Sci. Technol. 37, 4709–4716.

Zawislanski, P.T., Zavarin, M., 1996. Nature and rates of selenium transformations in Kesterson Reservoir soils: a laboratory study. Soil Sci. Soc. Am. J. 60, 791–800.

Zawislanski, P.T., Benson, S.M., TerBerg, R., Borglin, S.E., 2003. Selenium speciation, solubility, and mobility in land-disposed dredged sediments. Environ. Sci. Technol. 37, 2415–2420.

Zhang, Y., Moore, J.N., 1996. Selenium fractionation and speciation in a wetland system. Environ. Sci. Technol. 30, 2613–2619.